Ultrastructural Study on Experimental Infection of Rotavirus in a Murine Heterologous Model

Selma Majerowicz, Claire Fernandes Kubelka, Paulo Stephens, Ortrud Monika Barth

Departamento de Virologia, Instituto Oswaldo Cruz, Av. Brasil 4365, 21045-900 Rio de Janeiro, RJ, Brasil

Viral replication, histopathological and ultrastructural changes were observed for a period of nine days in the small intestine of suckling mice infected with a simian rotavirus (SA11). Samples taken from duodenum, jejunum and ileum were prepared for light microscopy, transmission and scanning electron microscopy analysis.

Histopathologic effect could be detected within 8 hr post-infection, when only a few altered cells were observed. Damage was extensive after 16 hr post-infection, showing swollen enterocytes and reduced and irregularly oriented microvilli at intestinal villi tips. Virus particles were detected at 16 and 48 hr post-infection, budding from the viroplasm into the rough endopl. mic reticulum cisternae in ileum enterocytes. Clear evidence of viral replication, observed by electron microscopy was not described before in heterologous murine models. Regeneration of the intestinal villi began at the third day post-infection.

Despite some differences observed in clinical symptoms and microscopic analysis of homologous and heterologous rotavirus infections, we concluded that mechanisms of heterologous rotavirus infection in mice follow similar patterns to those observed in the homologous models.

Key words: simian rotavirus - ultrastructure - heterologous model

Rotaviruses have been identified as the main ethiologic agent causing diarrhoeal disease in several animal species and humans (Estes et al. 1983, Muniappa et al. 1987, de Castro et al. 1988, Kapikian & Chanock 1990). Therefore various experimental animal models for rotavirus dissemination and for studies in vaccine development have been established.

Histological and electron microscope observations of experimental infections by homologous rotaviruses have been made in several models, such as mice (Adams & Kraft 1967, Banfield et al. 1968, Coelho et al. 1981, Starkey et al. 1986, Osborne et al. 1988, Ijaz et al. 1989), lambs (Snodgrass et al. 1979, Chasey & Banks 1986), calf (Mebus & Newman 1977), rats (Hu-ber et al. 1989) and piglets (Butler et al. 1974, Saif et al. 1978, Pearson & McNulty 1979, She-pherd et al. 1979, Narita et al. 1982, Theil et al. 1985).

The mouse model has been shown easy to handle and has reduced costs advantages. Experimental infections using heterologous rotaviruses in the mouse model reproduced the disease with human (Gouvea et al. 1986, Bell et al. 1987, Ebina et al. 1990), bovine (Ijaz et al. 1989) and simian rotavirus (Offit et al. 1984, Kubelka et al. 1994).

Received 15 December 1993
Accepted 30 May 1994

Ultrastructural studies using heterologous models in mice demonstrated morphological lesions in the villous epithelium (Gouvea et al. 1986) and virus particles inside the enterocytes of villous tips (Ijaz et al. 1989), without showing viral replication. This report describes sequential changes in intestinal cells and virus replication observed in mice infected with SA11 rotavirus, using light and electron microscope methods.

MATERIALS AND METHODS

Animals and virus infection - Swiss mice (SW 55) were originated from a colony maintained at the Biomedical Institute, Fluminense Federal University (Niterói, Brazil). The absence of serum antibodies to rotavirus sorotype A was confirmed by the enzyme immunoassay method.

Seven-day old mice were orally infected with 100 µl containing 4 x 10^5 PFU per animal of SA11 virus and were killed at 2, 4, 8, 16, 24 hr and 2 , 3, 5, 9 days post-infection (p.i.). Control mice were inoculated with uninfected MA-104 cells.

Segments of duodenum, jejunum and ileum were colected for viral RNA analysis and for virus detection in the faeces by negative staining electron microscopy and fixed for histological and cytological observations.

Polyacrilamide gel electrophoresis - The detection of SA11 virus nucleic acid in intestinal homogenates from infected mice was ac-

complished by a modification done by Pereira et al. (1983) in the method described by Laemmli (1970). The viral suspension obtained from infected mouse intestines and faeces was centrifuged and trypsin solution (10 µg/ml) was added to the supernatant. After incubation at 37°C for 30 min, MA104 cell monolayers were inoculated with 100 µl of each virus sample and adsorved at 37°C for 30 min. The inocullum was replaced with fresh Dulbecco's medium supplemented with trypsin (10 µl/ml), incubated at 37°C and daily observed. Cultures were frozen when cytophatic effect was observed. An aliquot of the infected cellular culture was incubated with 50 µl of 10% sodium dodecyl sulfate and 50 µl of 2 mg/ml of proteinase K at 37°C for 30 min. This mixture was then extracted with 500 µl phenol-chloroform V/V and centrifuged for 10 min at 12,000 g. The aqueous phase was separated and RNA was precipitated by addition of 50 µl of 20% NaCl and 1 ml ethanol at -20°C for 18 hr. The extract obtained was dried for 5 min in Speedvac or for 10 min in a dessecator. Then, 30 µl of the dissociating mixture was added and incubated for 15 min at 56°C. As control patterns rotavirus samples used were SA11 and EDIM. RNA detection was made by the method of silver nitrate staining described by Sammons et al. (1981) and modified by Herring et al. (1982).

Light microscopy (LM) - Semi-thin sections wee made from intestine samples previously embedded in Epon, stained with a methilene blue-azure II solution in phosphate buffer, pH 6.9, and a basic fucsin solution in 50% ethanol (Humprhey & Pittman 1974) and observed in a Zeiss Axiophot microscope.

Electron microscopy - For negative staining, 10 µl of guinea pig anti-rotavirus 1:100 diluted serum were added to 10 µl of the infected intestinal suspension and the mixture was incubated at 37°C for 30 min. Further 5 µl of a protein-A, colloidal gold linked solution, diluted 1:40 in PBS, were added and again incubated at 37°C for 30 min. A drop of this suspension was placed on carbon-coated Formvar grids, stained with 2% phosphotungstic acid (pH 7.2) and examined by transmission electron microscopy (TEM).

For scanning electron microscopy (SEM), intestine segments were fixed with 2% glutaraldehyde in 0.1 M phosphate buffer, pH 7.2. Segments were washed in phosphate buffer containing 7.2% sucrose, post-fixed in 1% osmium tetroxide, dehydrated in acetone, critical point dryed and coated with gold. Observations were made using a Zeiss DSM 940 scanning electron microscope.

For transmission electron microscopy, samples of the intestine were identically fixed and washed; they were dehydrated in graded acetone and embedded in Epon. Ultrathin sections were stained with uranyl acetate and lead citrate and examined with a Zeiss EM-900 electron microscope.

RESULTS

Clinical symptoms, viral RNA detection, and viral particles identification - The SA11 inoculated mice used for our ultrastructural studies showed first diarrhoeal symptoms at 24 hr post-infection. Most animals developed intense diarrhoea at 48 hr post-infection. By 72 hr post-infection, mice had recovered from diarrhoea. Genome analysis by eletrophoresis on polyacrylamide gels confirmed segment profiles characteristic of rotavirus SA11 (Fig. 1).

Immunoelectron microscopy, using the negative staining technique, confirmed rotavirus shape and antigenicity in the material recovered from infected mice (Fig. 2).

MORPHOLOGICAL OBSERVATIONS

Control animals - Light microscope observations of small intestine segments showed most villi regularly shaped. Granular vacuolation of the cytoplasm of villous epithelial cells was observed in the duodenum and jejunum (Fig. 3). Nuclei were found basal and regularly situated in all small intestine segments.

By scanning electron microscopy observations, villi are usually fingerlike shaped with round and smooth tips (Fig. 4). Apparently, their microvilli were equaly long (Fig. 5).

Transmission electron microscopy showed a well preserved layer of columnar epithelial cells, with long and regularly placed microvilli. The cytoplasm of these cells was dense, no necrotic elements were found and the usually oval shaped nuclei were placed at the basal region. The vacuolation observed in epithelial cells from control animals were always homogeneous, typical of the lactent age (Fig. 6). No loss of villous epithelial cells was observed.

INFECTED ANIMALS

Initial features of infection - Tissue and cell damage was not yet observed at 2 to 6 h.p.i. in most of intestinal villi. A few cells at the intestinal villous tips begun to be swollen and vacuolate at 8 h.p.i.

Viral replication stage - At 16 h.p.i, viral infection had already progressed. At light microscopy observation, intestinal villi remained long, but some enterocytes at the villous tips were markedly altered. Most cell nuclei remainned at the enterocytes cell basis. From 24 to 48 h.p.i. structural desorganization was evident, showing more intense and severe villous damage. Epithelial cells were rounded, shortned and swollen, mainly at the villous tips, sometimes dettached from adjacent cells and shed into the intestinal lumen (Fig. 7). Cells lost their nuclear polarity, showing increased apical vacuolation (Fig. 7). The destruction of villous tips and

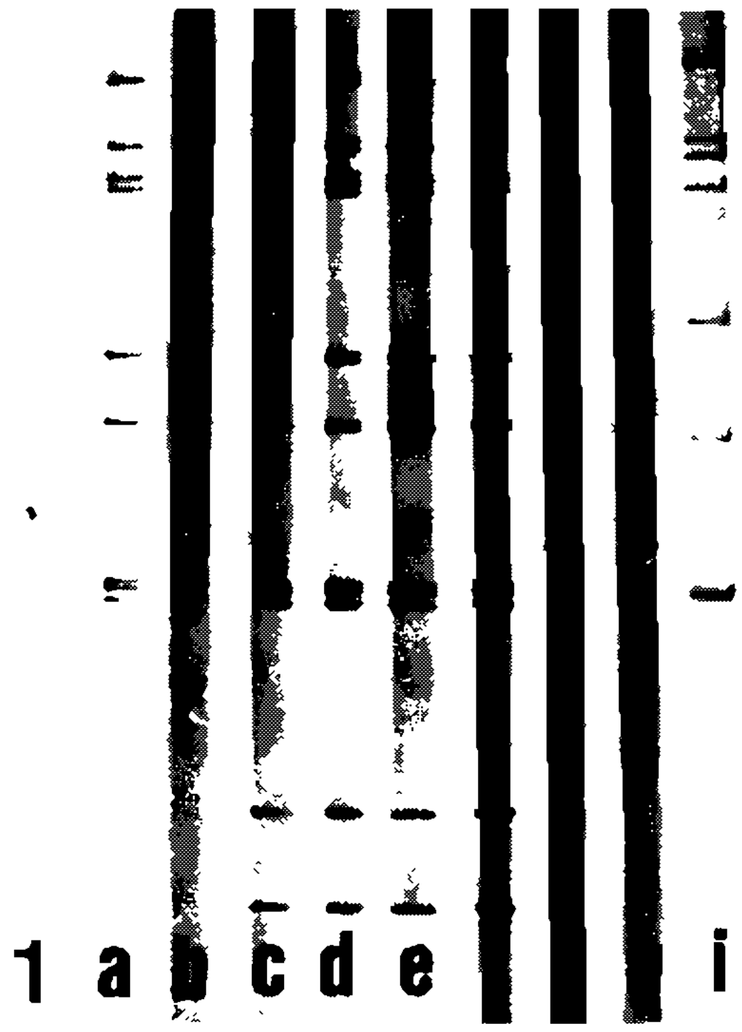

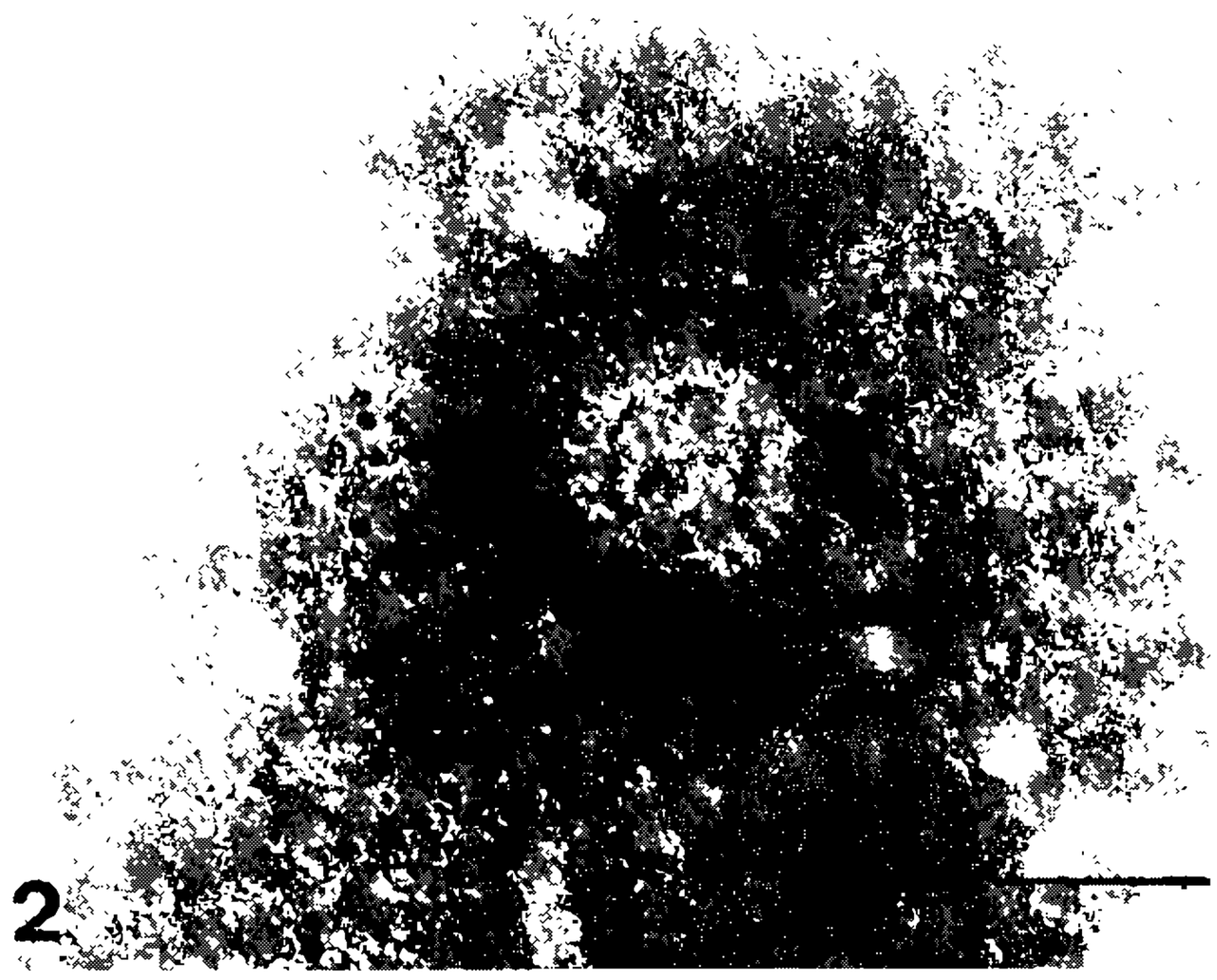

Fig.1: electrophoresis on polyacrylamide gels of rotavirus RNA. a: simian rotavirus SA11. b: control cell culture (MA104). c,d: cell culture with SA11 rotavirus of intestinal content of mice infected at 16 hr. e,f: cell culture with SA11 rotavirus of intestinal content of mice infected at 24 hr. g,h: cell culture with SA11 rotavirus of intestinal content of mice infected at 48 hr. i: murine EDIM rotavirus. Fig. 2: TEM - Immunoelectron microscopy, showing a viral particle labelled with guinea pig anti-rotavirus serum linked to protein A-colloidal gold conjugate, 250000 x. Bar= 60 nm. Figs 3-5: control animals. Fig. 3: LM - Intestinal villi showing absorptive cells with regular and basally placed nuclei, 400 x. Bar= 20 µm. Fig.4: SEM - Intestinal villi with smooth and regularly rounded tips, 520 x. Bar= 25 µm. Fig. 5: SEM - Microvilli of absorptive cells are long and regularly distributed, 5000 x. Bar= 2µm

moderate oedema in the *lamina propria* could be observed in all gut segments.

When observed by SEM, all villi appeared shortned with swollen or destroyed tips, confirming an extensive damage at 48 h.p.i (Fig. 8). Advanced pathologic effects were observed in all regions of the small intestine. Changes occured also in some villous absorptive cells at TEM level of resolution, whereas some other cells retained normal morphology (Fig. 9). Infected and damaged cells were markedly swollen, but there was no apparent discontinuity in the cell

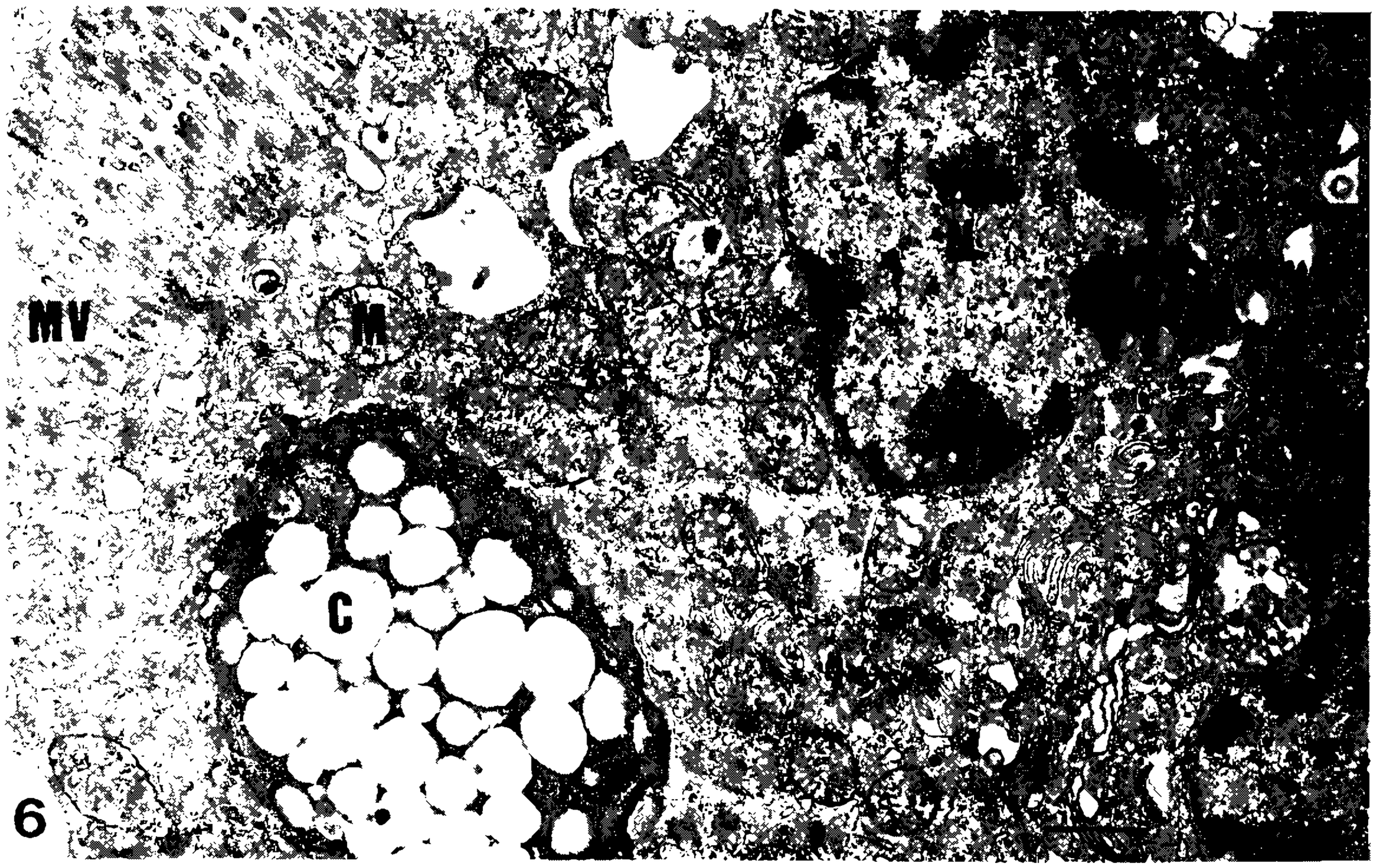

Fig. 6: TEM - Enterocyte of control suckling mouse, showing long and regularly distributed microvilli (MV), a dense cytoplasm, mitochondria (M) and homogeneous vacuolization, beside a goblet cell (C), 8800 x. Bar= 1 µm. Figs 7,8: infected animals. Fig. 7: LM - Villous tips showing some swollen epithelial cells (arrow), 400 x. Bar= 20 µm. Fig. 8: SEM - Intestinal shortened villi with destroyed tips, 300 x. Bar= 25 µm

membrane. The cytoplasm was vacuolated, rarefied and distended. Microvilli of variable length, thickness and shape were irregularly disposed and sometimes totally lost (Figs 9,13). Occasionally mitochondria appeared morphologically changed. These cells presented picnotic and irregular shaped nuclei.

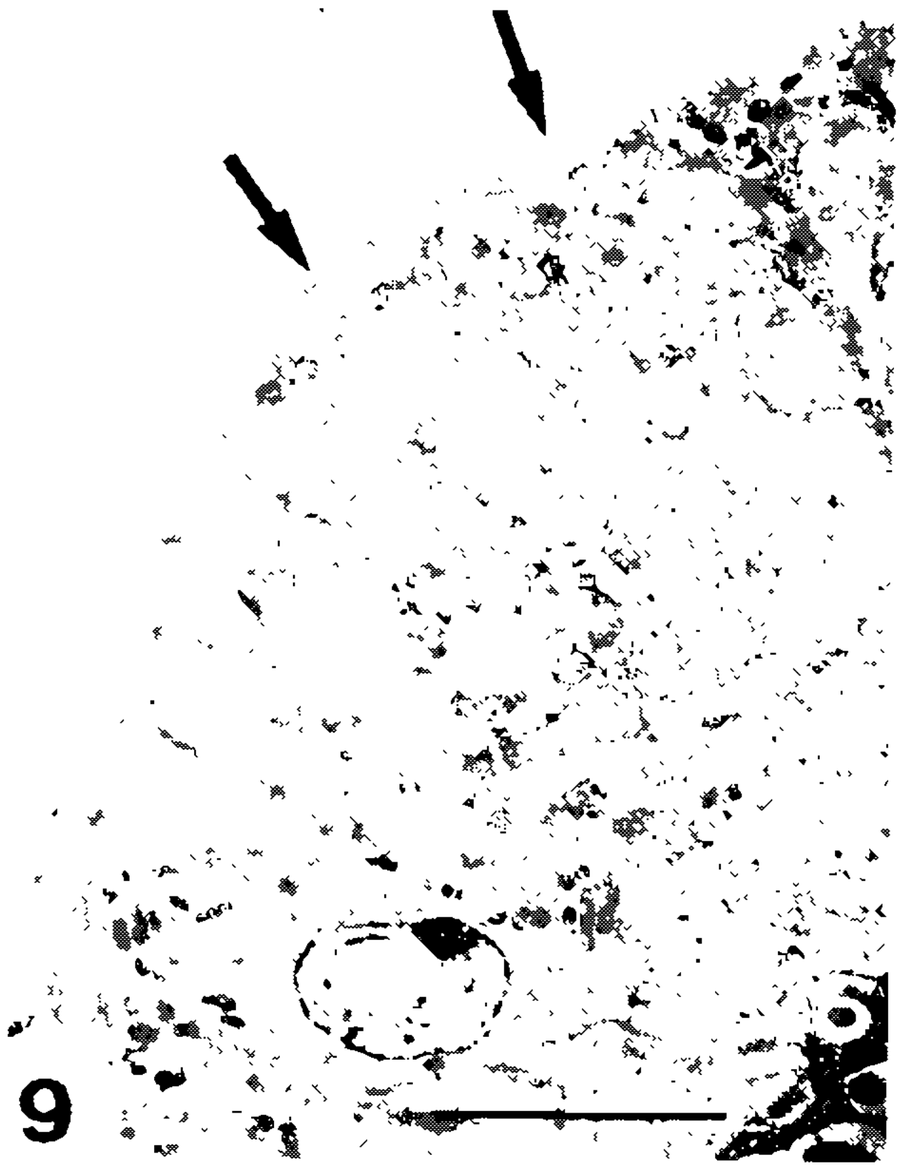

9

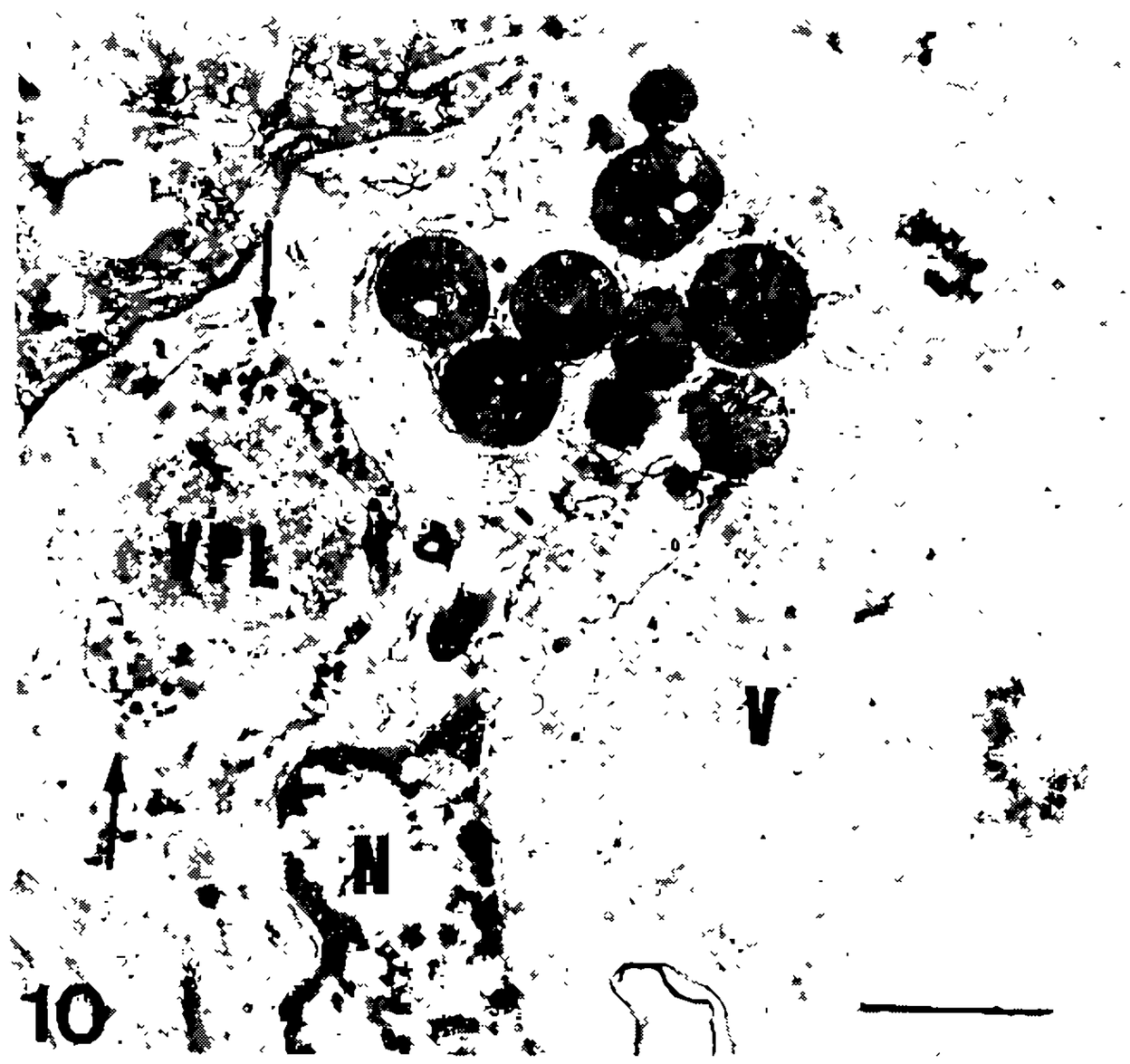

10

11

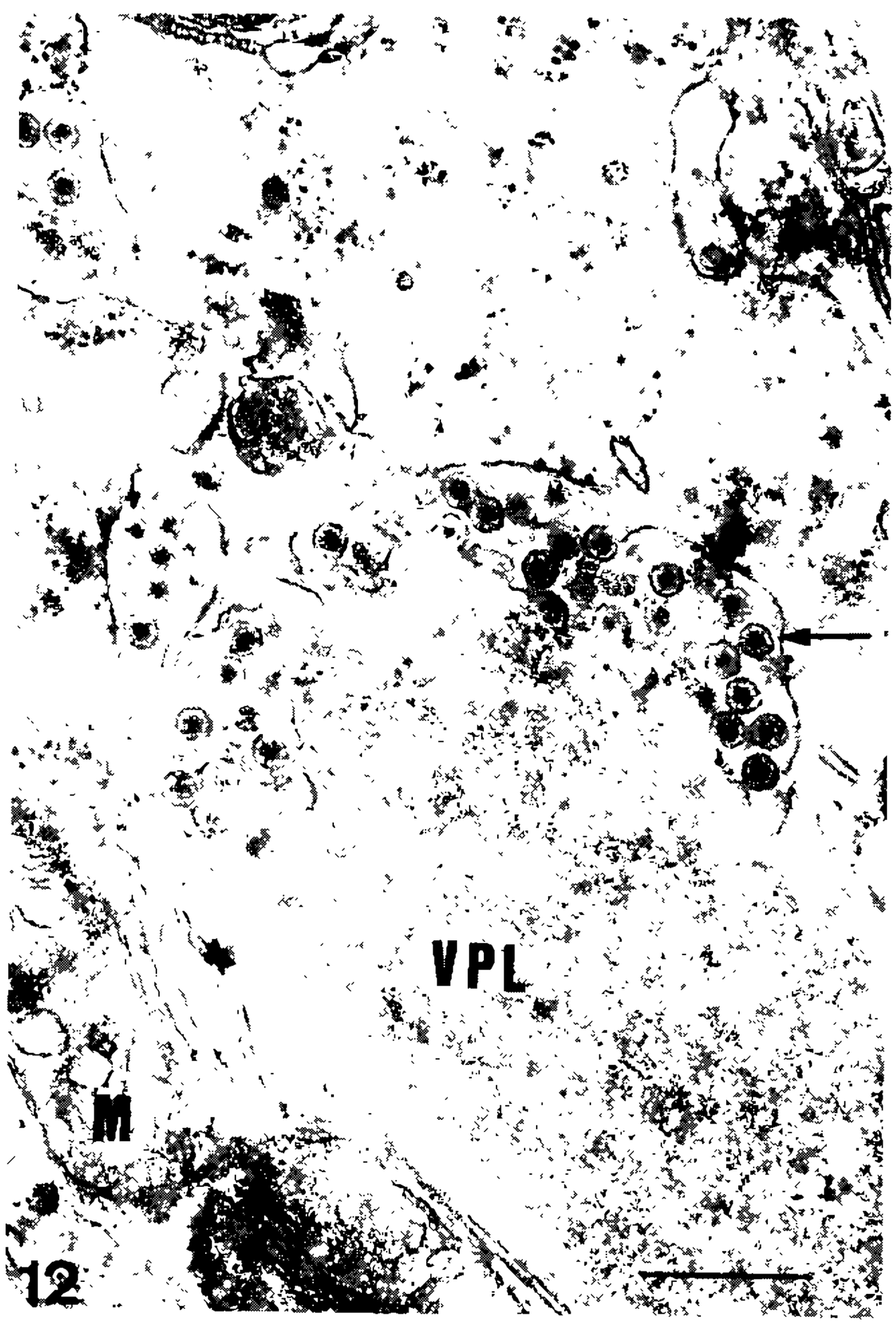

12

Figs 9-12: infected cells. Fig. 9 TEM - Intestinal villous showing some epithelial cells (arrows) morphologically changed, whereas others retain normal morphology (right side), 1800 x. Bar= 10 µm. Fig. 10: enterocyte with a viroplasm (VPL), showing virus particles inside the RER (arrows), nucleus (N) and a large vacuole (V), 11100 x. Bar= 1,2 µm. Fig. 11: TEM - Viroplasm with precursor particles (arrow), budding into the RER, V= vacuole, N= nucleus,19200 x. Bar= 0,5 µm. Fig.12: TEM - Viroplasm (VPL) showing particles type II (large arrow) and type III (small arrow) inside the RER, 31000 x. Bar= 0,5 µm.

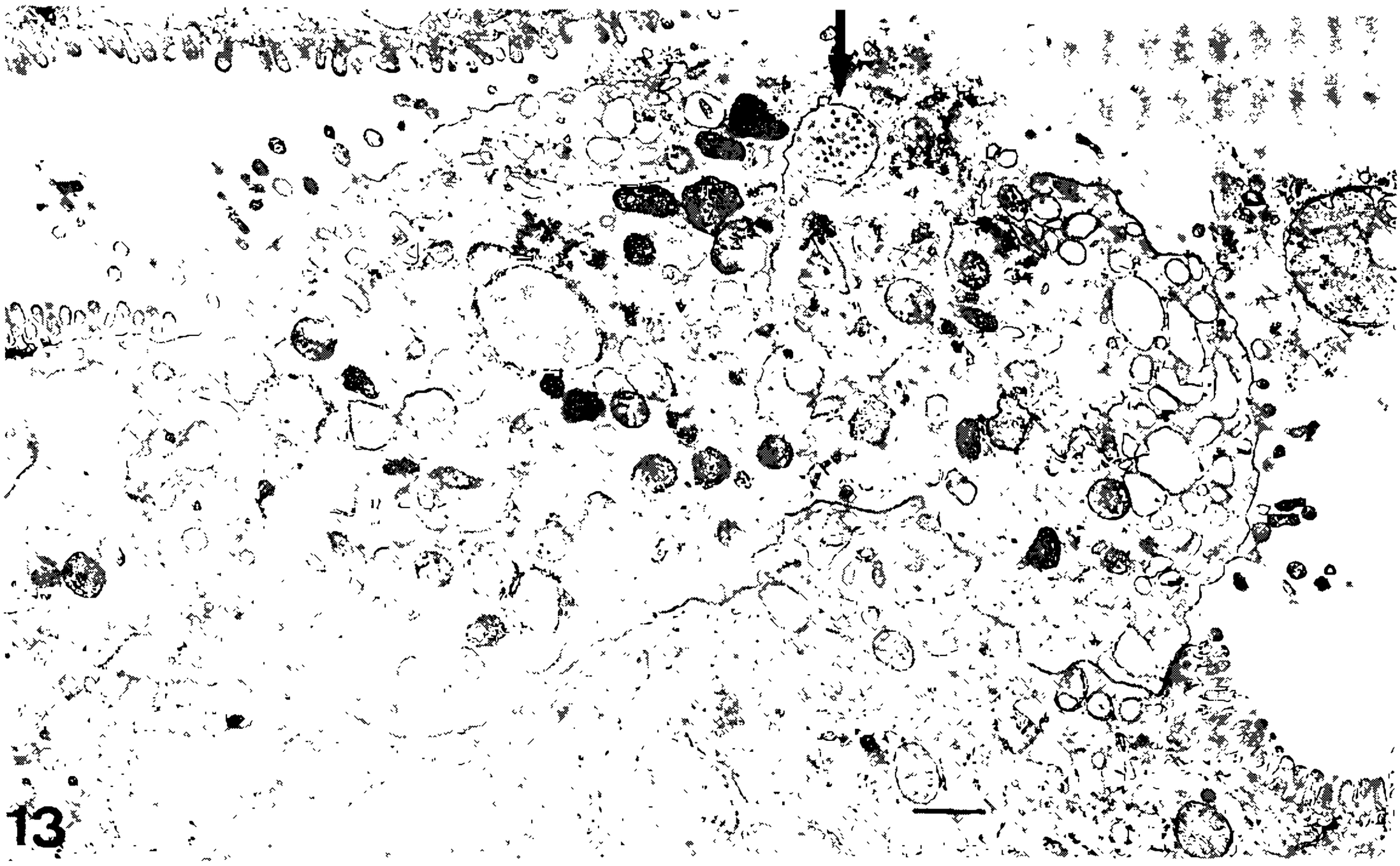

13

14

15

16

Fig. 13: TEM - Infected enterocyte at 48 hr showing viral particles shedding into the intestinal lumen, still inside RER vesicles (arrow), 7700 x. Bar= 1 μm. Figs 14-16: recovery step. Fig. 14: LM - Intestinal villi presenting no significative lesions, demonstrating tissue recovery at 72 hr, 200 x. Bar= 40 μm. Fig. 15: SEM - Villi do not show morphological alterations at 72 hr, 336 x. Bar= 25 μm. Fig. 16: SEM - A regenerated intestinal villous tip, nineth day post-infection: cell surfaces are covered by regularly disposed microvilli, 33870 x. Bar= 2 μm.

Viral particles were seldom detected inside ileum epithelial cells at 16 h.p.i., but their presence confirmed that viral replication occured (Fig. 10). Presumed virus precursor particles were associated with dense, amorphous viroplasm, from where they budded into the rough endoplasmic reticulum (Fig. 11). During this stage they picked up a portion of the RER - membrane as a virus particle transitory envelope. Inside the RER, enveloped putative viral particles were transformed in mature virus particles after loosing its transitory envelope, when they appeared more electron translucent with a smooth fuzzy coat. Enveloped particles with 70-80 nm and fuzzy coated particles with 50-70 nm in diameter were found together inside cisternae of the RER (Fig. 12). Afterward, groups of presumed virus particles, still inside RER vesicles were shedded into the intestinal lumen, together with some cellular content (Fig. 13).

Recovery step - Pathological analysis made by light microscopy at 72 h.p.i. did not detect any significative lesion at the small intestine segments, confirming tissue recovery. Villi had regular arquiteture; the enterocytes had granular vacuolation and nuclei showed basal polarity (Fig. 14). By SEM observation, no morphological changes of the intestinal villi were detected (Fig. 15), and enterocytes recovered their original shape (Fig. 16). Absorptive epithelial cells were not altered showing normal villi in all gut segments.

DISCUSSION

Pathology and viral replication of a simian rotavirus SA11 infection in an heterologous model of suckling mice were elucidated by ultrastructural observations.

Light microscopy data were similar to those described by Gouvea et al. (1986), Ijaz et al. (1989), Ebina et al. (1990) and Kubelka et al. (1994), also using heterologous models. Histopathological aspects of our model with a SA11 rotavirus were similar to the Epizootic Diarrhea of Infant Mice (EDIM) rotavirus (Adams & Kraft 1967, Coelho et al. 1981, Stephen 1988); however, EDIM persisted at least for seven days (Coelho et al.1981, Osborne et al.1988), while recovery from SA11 infection was observed at the third day p.i.

In our experiments, severe tissue damage occurred at 48 h.p.i.. General redution and destruction of intestinal villous tips were shown by light- (LM), scanning electron- (SEM) and transmission electron microscopy (TEM). These pathologic changes were observed also in mice infected with human rotavirus (Gouvea et al. 1986) and by porcine rotavirus in an homologous model (Theil et al. 1985). EDIM showed advanced lesions of intestinal villi (Coelho et al. 1981, Chasey & Banks 1986, Starkey et al. 1986), but severe villous atrophy as we observed was only described by Osborne et al. (1988) and Stephen (1988).

Syncytia of absortive epithelial cells have been described in atypical rotavirus infections (Mebus et al. 1978, Askaa & Bloch 1984, Vonderfecht et al. 1984, Chasey & Banks 1986, Vonderfecht et al. 1986, Huber et al. 1989). Nuclei with abnormal polarity and clustered together were here observed in enlarged cells by light and electron microscopy. True syncytia were never found, since cell membrane dissolution could not be detected.

Presumed virus particles localized between microvilli as well as within the enterocyte cytoplasm were observed at TEM by Ijaz et al. (1989) during bovine rotavirus infection in mice. Nevertheless, these findings can not be considered as true evidence of viral replication at the ultrastructural level. We observed virus particles budding from viroplasm already at 16 h.p.i., which we interpret as signs of active viral replication. Such phenomenum has not yet been described for heterologous murine experimental models.

The different types of presumed viral particles characterized in our experimental model are in agreement with the morphological types I, II and III established by Chasey (1977) and Petrie et al. (1981), Schulze and Schumacher (1984) and Poruchinsky and Atkinson (1991). They related the type III particles to the end-phase of viral assembly, which correspond to complete infectious virus particles. On the other hand, several authors (Banfield et al. 1968, Pearson & McNulty 1979, Coelho et al. 1981, Narita et al. 1982) claimed that particles budding from the viroplasm to the RER would be virions (type II) and would correspond to the double-shell (ds) rotavirus particles observed by negative staining; smaller particles (type III) would represent the single-shelled (ss) particles. Further observations using technics such as immunocytochemistry and *in situ* hybridization may better explain these stages of virus maturation.

ACKNOWLEDGMENTS

To Alexandre Fialho for the polyacrylamide gel electrophoresis and Maria da Penha Costa Rodrigues for the photographic reproductions.

REFERENCES

Adams WR, Kraft LM 1967. Electron microscopic study of the intestinal epithelium of mice infected with the agent of epizootic diarrhea of infant mice (EDIM virus). *Am J Pathol 51:* 39-60.

Askaa J, Bloch B 1984. Infection in piglet with a porcine rotavirus-like virus. Experimental inoculation and ultrastructural examination. *Arq Virol 80:* 291-303.

Banfield WG, Kasmic G, Blackwell JH 1968. Further observations on the virus of epizootic diarrhea of infant mice. An electron microscopy study. *Virol 36:* 411-421.

Bell LM, Clark HF, OBrien EA, Kornstein MJ, Plotkin SA, Offit PA 1987. Gastroenteritis caused by hu-

man rotaviruses (serotype three) in a suckling mouse model. *Proc Soc Exp Biol Med 184:* 127- 132.

Butler DG, Gall DG, Kelly MH, Hamilton JR 1974. Transmissible gastroenteritis. Mechanisms responsible for diarrhea in an acute viral enteritis in piglets. *J Clin Invest 53:* 1335-1342.

Chasey D 1977. Different particle types in tissue culture and epithelium infected with rotavirus. *J Gen Virol 37:* 443-451.

Chasey D, Banks J 1986. Replication of atypical ovine rotavirus in small intestine and cell culture. *J Gen Virol 67:* 567-576

Coelho KIR, Bryden AS, Hall C, Flewett TH 1981. Animal model. Pathology of rotavirus infection in suckling mice: a study by conventional histology, immunofluorescence, ultrathin sections and scanning electron microscopy. *Ultrastruct Pathol 2:* 59-80.

De Castro L, Araujo HP, Gouvea VS, Pereira HG 1988. Serological evidence of rotavirus infection in a guinea pig colony. *Mem Inst Oswaldo Cruz 83:* 411-413.

Ebina T, Tsukada K, Umazu K, Nose M, Tsuda K, Hatta H, Kim M, Yamamoto T 1990. Gastroenteritis in suckling mice caused by human rotavirus can be prevented with egg yolk immunoglobulin (IgY) and treated with a protein-bound polysaccharide preparation (PSK). *Microbiol Immunol 34:* 617-629.

Estes MK, Palmer EL, Obijeski JE 1983. Rotaviruses: a review. *Cur Top Microbiol Immunol 105:* 124-168.

Gouvea VS, Alencar AA, Barth OM, de Castro L, Fialho AM, Araujo HP, Majerowicz S, Pereira HG 1986. Diarrhoea in mice infected with a human rotavirus. *J Gen Virol 67:* 577-581.

Herring AJ, Inglis NF, Ojeh CK, Snodgrass DR, Menzies JD 1982. Rapid diagnosis of rotavirus infection by direct detection of viral nucleic acid in silver stained polyacrilamide gels. *J Clin Microb 16:* 473-477.

Huber AC, Yolken RH, Mader LC, Stranberg JD, Vonderfecht SL 1989. Pathology of infectious diarrhea of infant rats (IDIR) induced by an antigenically distinct rotavirus. *Vet Pathol 26:* 376-385.

Humprey CD, Pittman EE 1974. A simple methylene blue-azureII-basic fuchsin stain for epoxi-embedded tissue sections. *Stain Technol 49:* 9.

Ijaz MK, Dent D, Babiuk LA 1989. Development of a murine model to study the pathogenesis of rotavirus infection. *Exper Mol Pathol 51:* 186-204.

Kapikian AZ, Chanock RM 1990. Rotaviruses, p. 1353-1397. In *Virology.* BN Fields, DM Knipe (eds). Raven Press, New York.

Kubelka CF, Marchevsky RS, Stephens PRS, Araujo HP, Oliveira AV. 1994. Murine experimental infection with rotavirus SA11: clinical and immunological characteristics. *Exper Toxicol Pathol* (in press).

Laemmli UK 1970. Clonage of structural proteins during the assembly of the head of bacteriophage T4. *Nature 227:* 680-685.

Mebus CA, Newman LE 1977. Scanning electron, light and immunofluorescent microscopy of intestine of gnotobiotic calf infected with reovirus-like agent. *Am J Vet Res 38:* 553-558

Mebus CA, Rhodes MB, Underdahl WR 1978. Neonatal calf diarrhea caused by a virus that induced villous epithelial cell syncytia. *Am J Vet Res 39:* 1223-1228.

Muniappa L, Georgiev KG, Dimitrov D, Mitouk B, Haralambiev EH 1987. Isolation of rotavirus from buffalo calves. *Vet Rec 120:* 23.

Narita M, Fucusho A, Shimizu Y 1982. Electron microscopy of the intestine of gnotobiotic piglets infected with porcine rotavirus. *J Comp Path 92 :* 589-597.

Offit PA, Clark HF, Kornstein MJ, Plotkin SA 1984. A murine model for oral infection with a primate rotavirus (Simian SA11). *J Virol 51:* 233-236.

Osborne MP, Haddon SJ, Spencer AJ, Collins J, Starkey WG, Wallis TS, Clark GJ, Worton KJ, Candy DCA, Stephen J 1988. An electron microscopic investigation of time-related changes in the intestine of neonatal mice infected with murine rotavirus. *J Pediatr Gastr Nutr 7:* 236-248.

Pearson GR, McNulty MS 1979. Ultrastructural changes in small intestinal epithelium of neonatal pigs infected with pig rotavirus. *Arq Virol 59:* 127-136.

Pereira HG, Azeredo RS, Leite JPG, Candeias JAN, Racz ML, Linhares AC, Gabbay YB 1983. Electrophoretic study of the genome of human rotavirus from Rio de Janeiro, São Paulo and Pará, Brazil. *J Hyg Camb 90:* 119-125.

Petrie Bl, Graham DY, Estes MK 1981. Identification of rotavirus particles types. *Intervirol 16:* 20-28.

Poruchynsky MS, Atkinson PH 1991. Rotavirus protein rearrangements in purified membrane-enveloped intermediate particles. *J Virol 65:* 4720-4727.

Saif LJ, Theil KW, Bohl EH 1978. Morphogenesis of porcine rotavirus in porcine kidney cell culture and intestinal epithelial cells. *J Genirol 39:* 205-217.

Sammons DW, Adams LD, Nishisawa EE 1981. Ultrasensitive silver-based color staining of polypeptides in polyacrilamide gels. *Electrophoresis 2:* 135-141.

Schulze P, Schumacher B 1984. Electron microscopic investigations of rotavirus morphogenesis in cell cultures. *Acta Virol 28:* 185- 190.

Shepherd RW, Butler DG, Cutz E, Gall DG, Hamilton JR 1979. The mucosal lesion in viral enteritis. Extent and dynamics of the epithelial response to virus invasion in transmissible gastroenteritis of piglets. *Gastroenterol 76:* 770-777.

Snodgrass DR, Ferguson A, Allan F, Angus KW, Mitchell B 1979. Small intestinal morphology and epithelial cell kinetics in lamb rotavirus infections. *Gastroenterol 76:* 477-481.

Starkey WJ, Collins J, Wallis TS, Clark GJ, Spencer AJ, Haddon SJ, Osborne MP, Candy DCA, Stephen J 1986. Kinetics tissue specificity and pathological changes in murine rotavirus infection of mice. *J Gen Virol 67 :* 2625-2634.

Stephen J 1988. Functional abnormalities in the intestine, p. 41-44. In *Viruses in the Gut.* MJG Farthing, Swan Press Ltd, London.

Theil KW, Saif LJ, Moorhead PD, Whitmoyer RE 1985. Porcine rotavirus-like virus (group B rotavirus): Characterization and pathogenicity for gnotobiotic pigs. *J Clin Microbiol 21:* 340-345.

Vonderfecht SL, Eiden JJ, Miskuff RL, Mebus CA, Yolken RH 1986. Identification of a bovine enteric syncytial virus as a nongroup A rotavirus. *Am J Vet Res 47:* 1913- 1918.

Vonderfecht SL, Huber AC, Eiden J, Mader LC, Yolken RH 1984. Infectious diarrhea of infants rats produced by a rotavirus-like agent. *J Virol 52:* 94-98.